Key words. Wavelets, Ornstein-Zernike equation, integral equations, multilevel method

Multilevel wavelet solver for the Ornstein-Zernike equation

M. V. Fedorov

Theory and Computation Group, Centre for Synthesis and Chemical Biology,
Conway Institute of Biomolecular and Biomedical Research,
Department of Chemistry, University College Dublin,
Belfield, Dublin 4, Ireland, email Maxim.Fedorov@ucd.ie

G. N. Chuev

Institute of Theoretical and Experimental Biophysics,
Russian Academy of Sciences, Pushchino, Moscow Region,
142290, Russia, email genchuev@rambler.ru

C. T. Kelley

North Carolina State University, Center for Research in Scientific
Computation and Department of Mathematics, Box 8205,
Raleigh, N. C. 27695-8205, USA, email Tim_Kelley@ncsu.edu

B. Montgomery Pettitt

University of Houston, Department of Chemistry,
Houston, TX 77204-5003, USA, email pettitt@uh.edu

Abstract

A multilevel wavelet algorithm is developed to solve integral equations for the pair correlations in simple liquids. The algorithm is based on the discrete wavelet transform of the radial correlation functions. The fundamental properties of wavelet bases are employed to improve the convergence and speed of the algorithm. The Coifman 2 basis set is used for the wavelet treatment. To solve the Ornstein-Zernike integral equations we have applied a combined scheme in which the coarse part of the solution is calculated with the use of wavelets by a multilevel method, and the fine part by Picard iteration. We report on numerical experiments which show that the proposed procedure is more effective than one in which the coarse grid solution is computed by a single-level iteration.

I. INTRODUCTION

Integral equation (IE) theories using the Ornstein-Zernike equation and its variants have proven to be a successful tool for treating simple liquids.[1] The IE method consists in calculating of the radial distribution function (RDF) by solving the set of equations formed by the Ornstein-Zernike (OZ) integral equation and a closure relation. The OZ equation relates the total pair correlation function $h(r)$ with the direct correlation function $c(r)$, for an isotropic liquid with density ρ. The OZ equation is a convolution integral equation given by:

$$h(r) = c(r) + \rho \int c(|\mathbf{r} - \mathbf{r}'|)h(\mathbf{r}')d\mathbf{r}'. \tag{1}$$

The closure relation couples the same quantities, h and c, and the interaction potential $U(r)$. Formally this relation may be written in terms of the indirect correlation function $\gamma(r) = h(r) - c(r)$ as

$$c(r) = \exp[-\beta U(r) + \gamma(r) + B(\gamma)] - \gamma(r) - 1, \tag{2}$$

where $\beta = (k_B T)^{-1}$ is the inverse of the temperature, T and the Boltzmann constant, k_B. The closure introduces the bridge function $B[\gamma]$ which is a nontrivial functional of γ.[1] Given $U(r)$, T, ρ, and an approximate $B[\gamma]$ the IE method consists in finding a solution to set (1)-(2). By solving the set all the required correlation functions and, hence, all the thermodynamic and structural properties of fluid may be obtained. Since the exact expression for $B[\gamma]$ is computationally intractable, approximation to the bridge function is a central aspect of contemporary IE theories. The list of such approximating closures is still expanding and includes, for example, $B[\gamma] = 0$ for the hypernetted chain (HNC) closure, $B[\gamma] = \ln(1 + \gamma(r)) - \gamma(r)$ in the Percus-Yevick approximation, etc. These approximations have been studied extensively for simple liquids, and their failure and advantages are well documented in literature.[1]

Although there are a few special cases when the integral equations can be solved analytically, numerical solutions of (1)-(2) are required for physically realistic choices of the potential, U. For numerical calculations the Fourier representation of the OZ equation

between c and γ is often useful:

$$\widehat{\gamma}(k) = \frac{\rho\hat{c}^2(k)}{1-\rho\hat{c}(k)}, \tag{3}$$

where $\hat{f}$ denotes the three-dimensional (3D) Fourier transform (FT) of f. In the radially symmetric case considered in this paper, the FT reduces to to the one-dimensional (1D) spherical-Bessel transform $\hat{f}(k) = 4\pi/k \int_0^\infty r \sin(kr) f(r) dr$. The inverse Fourier transform $(\mathrm{FT})^{-1}$ can be obtained in a similar manner.

The conventional method is based on the Picard scheme and given an initial guess to the usually nonlinear IE uses direct iteration.[3, 17] Unfortunately several hundred iterations may be needed even for a rather accurate initial approximation of $\gamma(r)$. The Newton-Raphson (NR) algorithm [2] appears to be much more efficient, but when implemented in a naive way, requires calculation of the Jacobian matrix and the solution of the linearized problem.[3]

The conventional numerical schemes for solving IE suggest the solution to be divided into the "coarse" and "fine" parts and the algorithm to be a hybrid of the Newton-Raphson and Picard schemes for the coarse and fine parts, respectively.[3] The former being obtained as an expansion in the basis of roof functions [3] or plane waves [4]. Because this method does not directly address the computation or storage problems, special efforts are required to approximate and store the full Jacobian matrix to achieve a reasonable algorithm.

Another approach is to use a matrix-free iterative procedure, such as a Newton-Krylov or Newton-multigrid method [5, 6]. Here we employ a wavelet-based approach. To combine a Newton-multigrid method with wavelets would require additional algorithms (see, for example [7]), to use such an approach. Therefore, in this paper we will restrict ourselves only to an NR iteration with full coarse-grid matrix storage, and concentrate on the advantages of a special choice of basis set for the coarse solution, namely, wavelets. The results of the coupling of matrix-free solvers and a wavelet approximation will be a topic of future research.

II. NUMERICAL SCHEME BASED ON WAVELETS

A. Wavelet representation of the OZ equation

Wavelet analysis is a modern numerical tool that is an extension of Fourier analysis. There are many examples of wavelet techniques and their applications [8–12]. We restrict our consideration to the orthonormal and compactly supported wavelets. Details of wavelet applications to IE's are described in [13, 14]. Wavelets are functions which form an orthonormal basis for $L^2(R)$. Unlike the harmonic functions wavelets have dual localization characteristics in both the real and reciprocal spaces. Any square-integrable function $f(r)$ can be expanded as a sum of linear combinations of scaling functions at the chosen resolution $j = j_0$ and wavelet functions at all finer resolutions $j \geq j_0$:

$$f(r) = \sum_s a_{j_0 s}\varphi_{j_0 s}(r) + \sum_{j_0}^{\infty}\sum_s d_{js}\psi_{js}(r), \tag{4}$$

where the coefficients $\{a_{j_0 s}\}$ and $\{d_{js}\}$ are obtained by the inner product with appropriate basis functions:

$$a_{j_0 s} = \int f(r)\varphi_{j_0 s}(r)dr; \;\; d_{js} = \int f(r)\psi_{js}(r)dr. \tag{5}$$

Equation (4) is considered to be a discrete wavelet transform (DWT). In expansion of (4) the first term gives a "coarse" approximation of $f(r)$ at the resolution j_0 and the second term gives a sequence of refinements (details). In practice the details are cut off at the appropriate resolution desired $j_{\max}$. This means that we have a finite number of decomposition levels $L \equiv j_{max} - j_0$. We also truncate r to a finite interval by limiting the upper limit of the sequence of translates $\{s_i\}$ to a finite value S.

It should be mentioned that the number of terms can be different for the coarse and fine parts. Applying the algorithm of fast wavelet transform (FWT) to calculate the approximating coefficients [8], we can avoid the direct integration in (5). The elegant pyramidal procedure provides a low computational cost for such calculations.

To apply the wavelet technique to IE's we employ the wavelet representation of the OZ equation [14]. We briefly review the approach from [14] below.

We begin by decomposing the correlation functions into coarse and fine parts:

$$c(r) = c_c(r) + c_f(r), \quad \gamma(r) = \gamma_c(r) + \gamma_f(r). \tag{6}$$

Then, we express the coarse parts of the direct and indirect correlation functions in terms of the chosen wavelet scaling functions with the appropriate number of resolution levels L as:

$$\gamma_c(r) = \sum_s G_{Ls}\varphi_{Ls}(r), \qquad c_c(r) = \sum_{s'} C_{Ls'}\varphi_{Ls'}(r). \tag{7}$$

We denote the set of approximating coefficients $\{G_{Ls}\}$, and $\{C_{Ls'}\}$, as the vectors–columns $\mathbf{G_L}$, and $\mathbf{C_L}$ respectively. In general the relevant coefficients are found by the inner product of $c(r)$ or $\gamma(r)$ with the scaling functions $\{\varphi\}$ similar to (5). We use a FWT to find them in this work.

We introduce the convolution matrices $\mathbf{W_L}$ whose elements are given as:

$$W_L(s, s', m) = \int \varphi_{Lm}(r)dr \int \varphi_{Ls}(|\mathbf{r} - \mathbf{r}'|)\varphi_{Ls'}(r')d\mathbf{r}'. \tag{8}$$

We can see that each one-dimensional subset $W_L(s, s', :)$ is the set of the scaling functions coefficients of the wavelet transform (5) for the convolution product $D_L^{ss'}$:

$$D_L^{ss'} = \int \varphi_{Ls}(|\mathbf{r} - \mathbf{r}'|)\varphi_{Ls'}(r')d\mathbf{r}'. \tag{9}$$

We define a matrix $\mathbf{A_L}$ and a column–vector B_L whose elements are defined as:

$$A_L(:, m) = \mathbf{C_L}^T \cdot W_L(:, :, m), \quad B_L(m) = \sum_{k,l}[\mathbf{C_L} \cdot \mathbf{C_L}^T] \odot W^L(:, :, m), \tag{10}$$

where the upper index T denotes the transposition, symbol " $\cdot$ " denotes the matrix product, " $\odot$ " denotes the dot product of two matrixes and " : " means a subset of a matrix in one dimension. In Eq. (8) the convolution matrix $\mathbf{W_L}$ depends only on the choice of the wavelet basis set and chosen number of decomposition levels and has to be evaluated only once before the calculation of the correlation functions and then stored in the computer memory. One might think that the cost of computing W_L is large enough to make this approach impractical. However, this cost is only incurred on the coarse mesh, can be amortized over many computations, and, using properties of the wavelet basis, W_L can be well approximated by an extremely sparse matrix which can itself be computed using the nodal values of $D_L^{ss'}$ (see § II B).

Making the wavelet transform of the left and the right parts of the (1) and taking into account the wavelet orthogonality, we obtain the wavelet representation of the OZ equation for the coarse parts of the chosen level L:

$$\mathbf{G}_L = \rho\,[\mathbf{I} - \rho \cdot A]^{-1} \cdot B, \tag{11}$$

where $\mathbf{I}$ is the unity matrix, while $[\mathbf{I} - \rho A]^{-1}$ is the matrix inverse to $[\mathbf{I} - \rho A]^{-1}$. Using the inverse FWT we can reconstruct $\gamma_c(r)$ from the set of coefficients $\mathbf{G_L}$. As the fine parts of the correlation functions are assumed to be zero for the initial step we restrict (2) to the coarse level and obtain

$$c_c(r) = \exp[-\beta U(r) + \gamma_c(r) + B[\gamma_c]] - \gamma_c - 1. \tag{12}$$

Using FWT we perform the wavelet transform of $c_c(r)$ to obtain the set of $\mathbf{C_L}$ and use it as a next input for (11).

Thus, our numerical scheme proposes the following cycle for obtaining the coarse solution:

$$\mathbf{G_L}^{in} \to (FWT)^{-1} \to \gamma_c(r) \to (12) \to (c_c) \to (FWT) \to \mathbf{C_L} \to (11) \to \mathbf{G_L}^{out}, \tag{13}$$

If the number of wavelet coefficients is not relatively large, the solution of (11) with direct and back FWT requires less computation than the direct and the back FFT at each iteration.

When the required accuracy is achieved we start the second loop for calculating the fine part $\gamma_f(r)$. For this purpose we consider the coarse part $\gamma_c(r)$ as an initial approximation for $\gamma(r)$ at the second loop. Then starting from this approximation we perform the calculations by direct iterations:

$$\gamma^{in}(r) \to (2) \to c(r) \to (FFT) \to \widehat{c}(k) \to (1) \to \widehat{\gamma}(k) \to (FFT)^{-1} \to \gamma^{out}(r). \tag{14}$$

If the coarse solution is rather closed to the true one the number of direct iterations is not so large and does not usually exceed 20-30. The efficiency of the method depends on the number of approximating coefficients. Due to the special choice of the wavelet basis this number can be rather small, providing rapid convergence.

As was previously shown[13, 14] this method allows us to solve integral equations for simple and molecular liquids with less computational effort than the conventional methods

of integral equations theory. But as we will show in the next section the speed and the convergence of this method can be strongly improved using the fundamental properties of wavelets and radial correlation functions in a multilevel scheme.

B. Multilevel approach to finding the coarse solution

Although the scheme described above is significantly faster than conventional methods, we still have to pay for direct and back FWT transform which costs about $O(N)$ for each cycle, where N is the size of the coarse grid.

Fortunately we have a route to avoid these operations. Note that functions $\gamma(r)$ and $c(r)$ are quite smooth in most of practical cases (i.e. non hard sphere potentials etc). Thus, these functions have at least second derivative in the segment $]0, \infty]$. In this case we can employ the fact that for several wavelet families such as Coifman and Hyperbolic wavelets [16] the coefficients of the wavelet expansion of a function $f(x)$ can be estimated directly from the values of the function itself. The estimation error depends mainly on the basis set and number of derivatives [9, 10, 15]. In fact, we can also estimate the values of reconstructed function at the nodes directly from the wavelet coefficients. In our case it means that we can estimate the values of $\mathbf{C_L}$ using the relationship (12) as:

$$C_{Ls} \approx exp(-\beta U(sd_L) + KG_{Ls} + B(KG_{Ls})/K - G_{Ls} - 1/K, \tag{15}$$

where the d_L is a distance between nodes at the level L and K is a constant. These values depend only on a particular implementation of the FWT algorithm. In our case the $d_L = d2^L$ where d is the size of grid in the finest level of resolution. The constant K is equal to $2^{-L/2}$. So we can avoid the direct and back FWT in the cycle (13) and simplify our scheme.

$$\mathbf{G_L}^{in} \rightarrow (15) \rightarrow (\mathbf{C_L}) \rightarrow (11) \rightarrow \mathbf{G_L}^{out}, \tag{16}$$

We also use this approach for the calculations of the matrix $\mathbf{W_L}$. As was mentioned above, each column $W_L(k, l, :)$ of the matrix $\mathbf{W_L}$ is just the set of approximation coefficients of the wavelet transform applied to the convolution product $D_L^{ss'}$ (9) of the two scaling functions φ_{Ls} and $\varphi_{Ls'}$. Thus similar to (15) we can employ the following approximation:

$$W_L(s, s', m) \approx D_L^{ss'}(md_L)/K. \tag{17}$$

This significantly reduces the cost of computing $\mathbf{W_L}$ because we avoid $S \times S'$ number of FWT operations (S and S' are the numbers of coefficients for the coarse parts of correlation functions (7)).

To improve the convergence of this method we use a nested iteration, which is part of the multilevel strategy [17]. The main idea is that instead of the one number of decomposition levels L we choose the set of consecutively decreasing numbers $\{L_n\} : L_1 > L_2 > \cdots > L_n > \cdots > L_N \geq 0$. The zero value of L would correspond to the finest level of resolution (finest grid). The coarse solution obtained with the number of levels L_n serves as input for the next more accurate solution with L_{n+1} which serves as input for the next number L_{n+2} etc.

C. Details of calculations

To illustrate our scheme we have investigated an isotropic Lennard-Jones fluid with the interaction potential $U(r)$ given by $U(r) = 4\epsilon[(\sigma/r)^{12} - (\sigma/r)^6]$, where σ and ϵ are the size and energy parameters, respectively. The coarse approximations were found iteratively by (16) with three consequent resolution levels $[L_1 = 6, L_2 = 4, L_3 = 2]$. For each L the coarse solution was found until the required accuracy was achieved. For L_1 we used 20 wavelet coefficients for both sets $\mathbf{G_1}$ and $\mathbf{C_1}$. For L_2 and L_3 we used 50 and 100 coefficients respectively. The precision parameter for the numerical solution was equal to 10^{-4}.

To generate wavelets we used a grid with the number of points $n = 2048$ and step size $\delta r = \sigma/120$. For the first number L_1 we used the Newton–Raphson algorithm to improve convergence. For the numbers L_2 and L_3 we used a simple Picard scheme as the convergence was quite good. Jacobian matrices were calculated only on the coarse mesh.

It should be also mentioned that only $5-7$ Newton iterations were needed in this case to reach a good level of precision (see Fig. 1). We can see from that picture that to achieve a level of precision of about $10^{-10} - -10^{-11}$ we need only 7 iterations. The number of Picard iterations were increased almost by twice (from 38 to 72) when we decreased the termination parameter from 10^{-4} to 10^{-6}. Then the dependence of the number of iterations needed for convergence is linear in log-normal coordinates. So we pay about $18-19$ iterations for each next order of precision.

Concerning the choice of the wavelet basis set, we note that there are several common

sets such as Coifman, Hyperbolic, etc [10, 16] which can be used to realize the described scheme. We have used the Coifman (C2) set. The main feature of the Coifman basis is that the scaling function $\varphi(r)$ has the maximum number of vanishing moments at the fixed support. The larger the ratio of vanishing moments to the length of support, the better is the approximation of the first peak for the studied RDF [10].

Hence, using the C2 wavelets we can accurately treat an RDF with relatively sharp peaks. On the other hand, the C2 wavelets are rather smooth and well approximate the RDF within the ranges between these peaks. In addition this bases set had been already tested in the different applications involving IE's. [13, 14, 18].

The evaluation of the convolution product (9) can be easily performed in the case of radial wavelets, where the convolution can be evaluated via one-dimensional Fourier transforms (3) of the relative scaling functions. Moreover, the most of the coefficients (8) are nullified due to symmetry of the convolution and the compressive properties of FWT's for integral operators. According to [15], we can ignore all the coefficients which which are less than a constant M. We choose $M = 10^{-5}$ and found that it provides accurate calculations of correlation functions. For all the densities we start from the wavelet coefficients equal to zero at the coarsest level L_1.

In addition we should mention that $\mathbf{W_L}$ depends only on the basis set and resolution level. Therefore we do not need to calculate $\mathbf{W_L}$ in each cycle (and in each run of program as well), rather we evaluate the matrix $\mathbf{W_L}$ only once and then save it as a file.

In general it is possible to create a data-base of these matrices. That is why we regard them as tabular data and do not take into account their calculation expenses.

III. RESULTS AND DISCUSSION

Using the IE method based on discrete wavelets we have solved the OZ integral equations for simple fluids. Only the HNC closure has been considered here but the results should hold for other related closures. The solution was obtained in a wide range of size and energy parameters forf the fluid. To reveal the effectiveness of our algorithm we compare the CPU time required for the calculations by the wavelets and the conventional IE method at the same level of precision. Regarding the wavelet technique we used these two methods described above. The first one (W1) is based on the cycle (13) with forward and back

FWT's and a single value of $L = 4$. The second one (W2) is based on the cycle (16) with parameters described in the previous section. Fig. 2 depicts the CPU time required to obtain the solution at various values of the dimensionless parameter $\beta\epsilon$.

As is seen, the difference in computational costs for both the wavelets methods is small at low values of $\beta\epsilon$ corresponding to high temperatures, but the effectiveness of the W2 algorithm strongly increases as temperature decreases. This is due to that fact that this scheme is not sensitive to initial data and hence to the step $\delta(\beta\epsilon)$ even at high values of $\beta\epsilon$. Apart from this, the FWT-based W1 and the conventional one demand the results obtained at the nearest low value of $\beta\epsilon$ as the initial guess. Thus the computational expenses rise quite rapidly for the both methods. It should be mentioned that at low temperatures the conventional IE scheme requires a more accurate initial estimate leading to decreased step $\delta(\beta\epsilon)$. As a result, the computational expense of the wavelet scheme W1 is intermediate between the conventional Picard and the W2 schemes. A similar situation takes place also at high values of liquid density ρ.

Acknowledgments

The research of CTK was partially supported by National Science Foundation grants DMS-0070641, DMS-0209695, and DMS-0404537. BMP gratefully acknowledges NIH, the R.A. Welch foundation, and TIMES, funded by NASA Cooperative Agreement No. NC-1-02038 for partial financial support of this work.

---

[1] J.-P. Hansen and I.R. McDonald, *Theory of Simple Liquids. 2-nd ed.* (Academic, London, 1986).

[2] G. Zerah, J. Comput. Phys. **61** (1985) 280.

[3] M.J. Gillan, Mol. Phys. **38** (1979) 1781.

[4] S. Labik, A. Malijevsky, and P. Vonka, Mol. Phys. **56** (1985) 709.

[5] C.T. Kelley, *Iterative Methods for Linear and Nonlinear Equations.* Frontiers in Applied Mathematics, vol. 16, (SIAM, Philadelphia, 1995).

[6] C.T. Kelley, *Solving Nonlinear Equations with Newton's Method*, Fundamentals of Algorithms, vol. 1, (SIAM, Philadelphia, 2003).

[7] D.A. Knoll and D.E. Keyes, J. Comput. Phys. **193** (2004) 357.

[8] S.G. Mallat, *A Wavelet Tour of Signal Processing* (Academic press, San Diego, 1999).

[9] Y. Meyer, *Wavelets: Algorithms and Applications.* (SIAM, Philadelphia, 1993)

[10] I. Daubechies, *Ten Lectures on Wavelets.* CBMS/NSF Series in Applied Math. No. 61 (SIAM, Philadelphia, 1992).

[11] D.L. Donoho, Appl. Comput. Harm. Anal. **1** (1993) 100.

[12] R.T. Ogden, *Essential wavelets for statistical applications and data analysis.* (Birkhauser, Boston, 1997).

[13] G.N. Chuev, M.V. Fedorov, J. Comp. Chem. **25** (2004) 1369.

[14] G.N. Chuev, M.V. Fedorov, J. Chem. Phys. **120** (2004) 1191.

[15] G. Belkyn, R. Coifman, and V. Rokhlin, Comm. Pure and Appl. Math. **44** (1991) 141.

[16] R.A. DeVore, S.V. Konyagin, and V.N. Temlyakov, Constr. Approx. **14** (1998) 1.

[17] C.T. Kelley, B.M. Pettitt, J. Comput. Phys. **197** (2004) 491.

[18] G.N. Chuev, M.V. Fedorov, Phys. Rev. E **68** (2003) 027702.

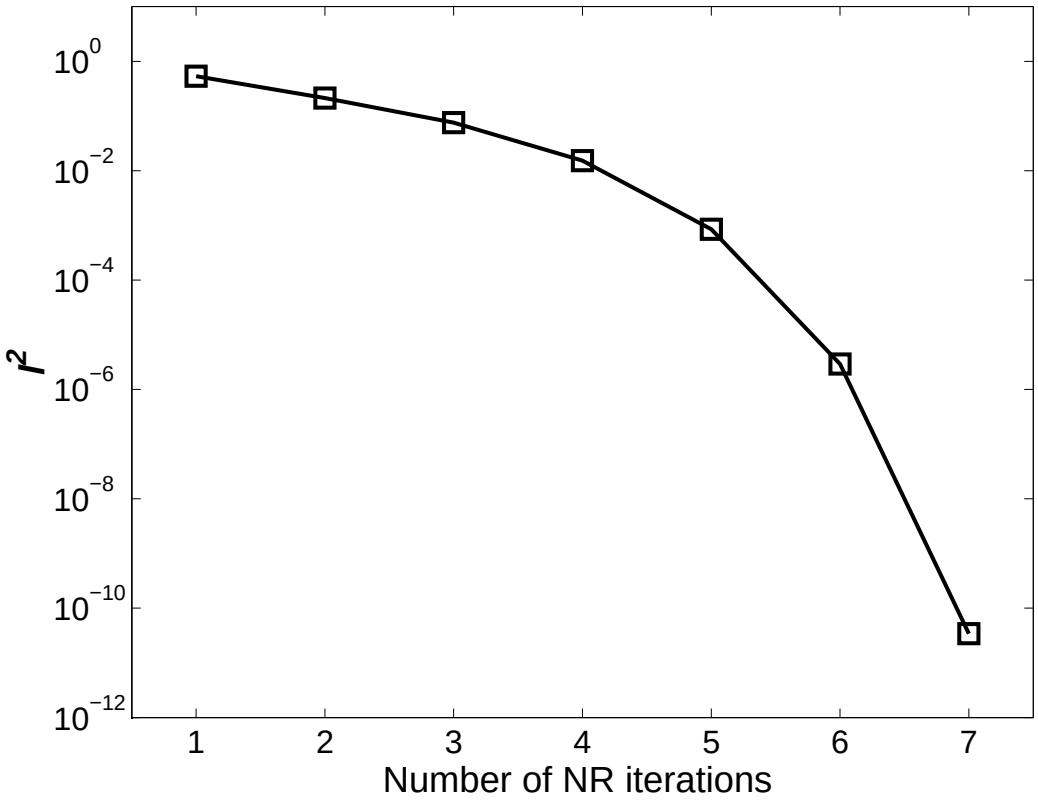

FIG. 1: The dependence of scaled l-square norm l^2 of discrepancy with regard to the number of NR iterations with the coarse mesh. The parameters of OZ equation are: $\beta\epsilon = 1$, $\rho\sigma^3 = 0.6$. The l^2 is in log scale.

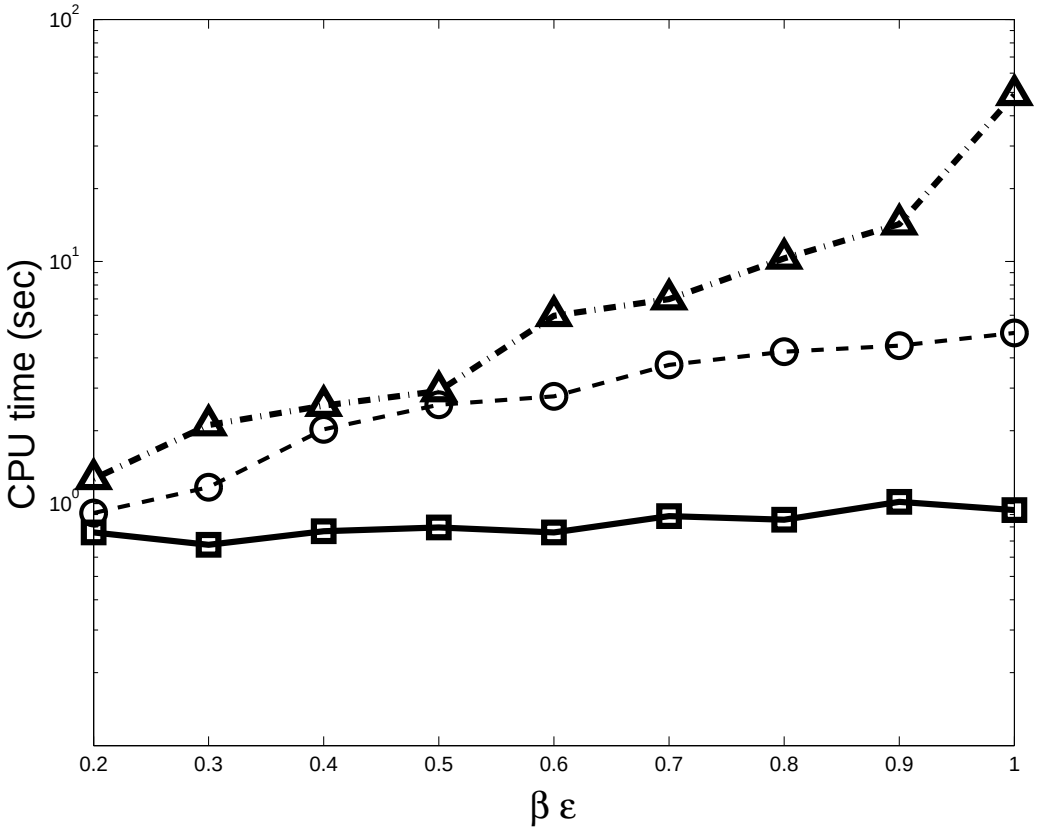

FIG. 2: CPU time (sec) required to obtained the solution by the wavelets methods W1 (circles, dashed line), W2 (rectangles, solid line) and by the conventional method (triangles, dash-dotted line) with versus parameter $\beta\epsilon$ at $\rho\sigma^3 = 0.6$. The CPU time is in log scale.